2.11 Measurement of Neutron-Production Double-Differential Cross Sections for Continuous Neutron-Incidence Reaction up to 100 MeV

Satoshi KUNIEDA[1]*, Takehito WATANABE[1], Nobuhiro SHIGYO[1], Kenji ISHIBASHI[1], Daiki SATOH[2], Yosuke IWAMOTO[3], Takashi NAKAMURA[4] and Robert C. Haight[5],

[1]*Department of Applied Quantum Physics and Nuclear Engineering, Kyushu University*
[2]*Japan Atomic Energy Research Institute*
[3]*High Energy Accelerator Research Organization*
[4]*Cyclotron and Radioisotope Center, Tohoku University*
[5]*LANSCE-3, Los Alamos National Laboratory*

The inclusive measurements of neutron-incident neutron-production double-differential cross sections in intermediate energy range is now being carried out Spallation neutrons are used as incident particles. As a part of this, the experiment was performed by using of NE213 liquid organic scintillators to detect outgoing-neutrons. Incident-neutron energy was determined by time-of-flight technique, and outgoing-neutron energy spectrum was derived by unfolding light-output spectrum of NE213 with response functions calculated by SCINFUL-R. Preliminary cross sections were obtained up to about 100 MeV, and were compared with calclations by the GNASH code. It will be hoped to get pure measurements by using of measured response functions for our detectors used in this study.

I. Introduction

Nuclear reaction data especially for neutrons and protons are required in the intermediate energy region for programs of accelerator driven transmutation system, radiotherapy, and space development Because it is difficult to get many measurements in this energy region, model calculations have been playing the major role. For example, calculation codes such as the GNASH[1)] based on the exciton and Hauser-Feshbach statistical model, NMTC/JAM[2)] based on the intranuclear-cascade-evaporation model, and the JQMD[3)] based on the quantum-molecular-dynamics had developed to get cross sections. Several measurements of double-differential cross sections (DDX) for proton-incident neutron-production have been reported in the wide intermediate energy region,[4-11)] and have been used to get reliabilities of model calculation, and/or to improve the models themselves. On the other hand, neutron-incident DDX measurements are very scarce in the intermediate energy region (Only a few of measurements[12,13)] had reported for neutron-production DDXs above about 20 MeV) It is difficult to get reliabilities on the model calculations for neutron-incidence

The purpose of this study is to measure neutron-production DDXs for neutron-incidence in the wide intermediate energy range by using of spallation neutrons as incident particles Liquid organic scintillators were used to detect outgoing-neutrons, and the fission chamber was used to know the number of incident-neutrons. Incident-neutron energy was determined by the time-of-flight (TOF) between the neutron source and neutron detectors Outgoing-neutron energy spectrum was obtained by unfolding charge-integration spectrum with calculated response functions of the detector Preliminary results were compared with the model calculations by the GNASH code

II. Experiment

1. Neutron source and neutron beam line

The experiment was performed at the 4FP15L beam line of WNR facility[14)] in Los Alamos Neutron Science Center (LANSCE). The schematic view of the neutron source and the neutron beam line used in this study is shown in **Fig. 1** Intense white neutrons covering up to about 750 MeV were provided from the Target-4 area where spallation reactions were triggered on the thick tungsten target by the part of the high-current (about 2 μA) 800 MeV proton beam from linear accelerator. This neutron beam line was 15° angled to the direction of the proton beam incidence, and was about 90 m long To decrease the number of low-energy (up to several tens

* Corresponding author, Tel +81-92-642-3765, Fax +81-92-642-3769, E-mail kuni@meteor nucl kyushu-u ac jp

MeV) neutrons from the Target-4 area, a polyethylene block of 101.6 mm thick was placed upstream on the beam line. Neutron flux was introduced into the the detector room through iron collimators of 35.7 mm in diametor that defined the beam size

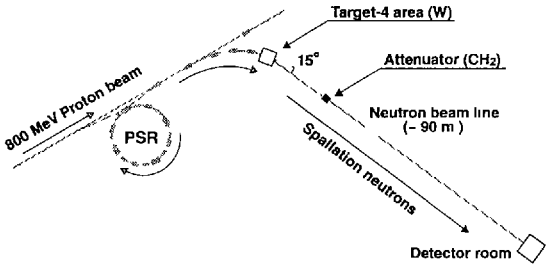

Fig. 1 Schematic view of the neutron source and the 4FP15L neutron beam line at WNR facility in LANSCE

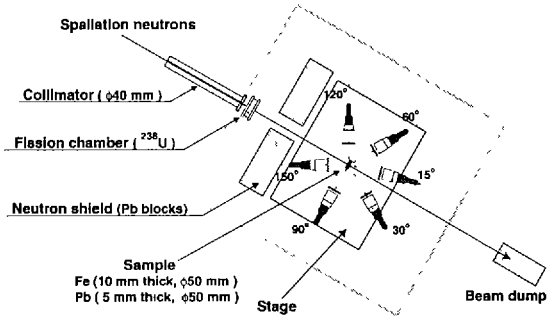

Fig. 2 Schematic view of the experimental setup

2. Experimental setup

The layout of the experimental arrangement is shown in **Fig. 2**. Cylindrical NE213 liquid organic scintillators were arranged at 15°, 30°, 60°, 90°, 120°, and 150° to detect outgoing-neutrons. The size of all these detectors were 127 mm thick and 127 mm in diameter, and were optically connected with photomultipliers. The average distance between the sample and detectors was about 0 7 m NE102A plastic scintillators of 10 mm thick were also set in front of all NE213 detectors to reject charged-particle events. To obtain the number of incident netrons, the fission ionization detector[15] was set right behind the collimator. Iron (10 mm and 40 mm thick) and lead (5 mm thick) were selected as samples. All of these samples were of natural compositions.

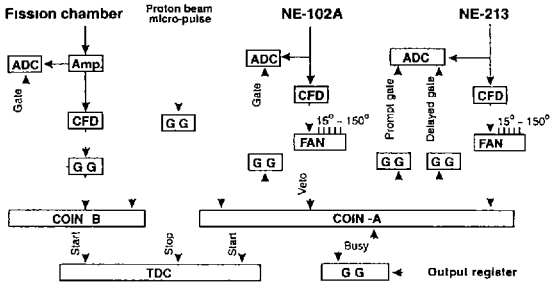

Fig. 3 Schematic draw of the electical circuit for online data aquisitions

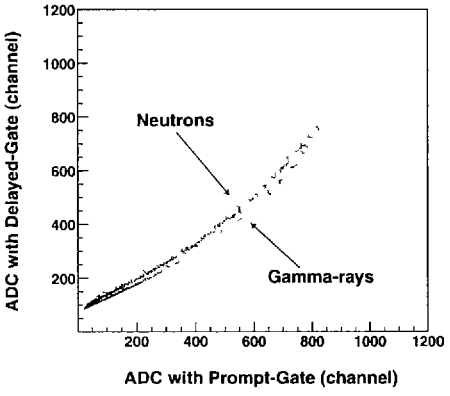

Fig. 4 Example scatter plot for charge-integrations with the prompt-gate and the delayed-gate for NE-213

The schematic block diagram of electrical circuit for online data acquisitions is shown in **Fig. 3** Analog signals from all detectors were branched into two One of these was converted into logic signal by the constant-fractional-discriminator (CFD) for each detector, and was sent to the coincidence module (COIN) Proton beam micro-pulses were delayed about 2 8 μ sec , and their width was adjusted by the gate-generator (G G) to be able to accept coincidences with logic signals of detectors within the micro-pulse spacing The proton beam micro-pulse spacing was about 1 8 μ seconds The lower energy limit of the neutron energy that could be accepted at COIN -A and COIN -B was about 10 MeV To eliminate most of charged particle events, logic signals from the NE102A were used as veto signals at COIN -A Coincidence signals were issued from either COIN -A or COIN -B, and were sent to the time-to-digital converter (TDC) as the start signal for TOF measurement On the one hand, micro-pulses of proton beam (delayed about 2 μ seconds, this time interval corresponded to the maximum

range of TDC module used in this experiment) were used as the stop signal Charge-integrations of analog signals were also recorded by using of charge-sensitive analog-to-digital converters (ADCs) for all neutron detectors after coincidences were caused For signals from photomultipliers of NE213s, two kind of charge-integrations were recorded to discriminate neutrons and gamma-ray events using the two gate integration method [16] As shown in **Fig. 4**, neutron and gamma-ray events are separated successfully

3. Calibration

Charge-integration spectra were calibrated for all neutron detectos to get corresponding electron-equivalent light-output The γ-ray compton-edges of ^{60}Co and Pu-Be sources were used with the semi-empirical formula of Dietze et al [17] for low-energy parts For the calibrations of higher-energy neutrons, spallation neutrons (collimators of 1 mm in diametor was used to identify the one neutron event) were induced directly into all NE213s as shown in **Fig. 5**. Neutron energies were identified by TOF, and were possible to be converted into light-unit by the empirical equation by Cecil et al.[18] Maximum channels of ADC spectra were used as corresponding charge-integration values. The relationship between charge-integrations and electron-equivalent light-output for NE213 is shown in **Fig. 6**. This example is for the detector used at 15°

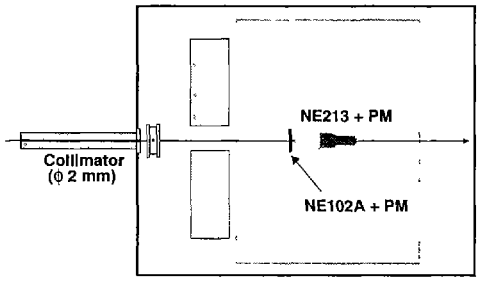

Fig. 5 Setup for the calibration of NE213 by using of spallation neutrons.

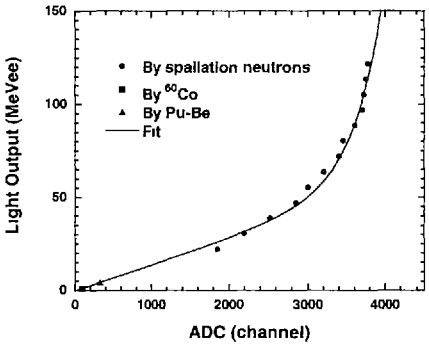

Fig. 6 Relationship between charge-integrations and electron-equivalent light-output for NE213

III. Analysis

1. Determination of incident neutron energy

Because raw data obtained in the online measurement were of whole events for overall incident energy range that were allowed in this data acquisition system, the incident-neutron energy was required to be identified for all outgoing-neutron evrents to get DDX In this study, incident neutron energies were determined by the TOF technique, on the assumption that the total TOF between the Target-4 and the neutron detector was exhausted only by the incident-neutron Because the flight path between the Target-4 and the sample (Time-B) was quite long enough to ignore the distance between the sample and all neutron detectors (Time-A), this assumption was acceptable Time-A and Time-B were estimated, and are compared in **Fig. 7** For example of 100 MeV neutron incidence, the ratio of time-A on time-B was not more than 3.5 % above about outgoing neutron energy of 5 MeV that correspond the lower energy limit of the n-γ discrimination

A typical TOF spectrum are shown in **Fig. 8** The sharp peak seen in this graph is flash gamma-ray events from the Target-4, and were used as the time fiducial to get TOFs of incident-neutron events Outgoing neutron events that were triggerd by incident-neutrons of the energy range above about 10 MeV were obtained in this measurement

2. Getting the number of incident neutrons

To normalize the outgoing-neutron spectrum, the number of incident neutrons must be known, and was possible to be gotten by the equation

$$N(E) = \frac{n_f(E)}{\sigma_f(E) \times \epsilon_{det} \times \rho_f} \tag{1}$$

where, $N(E)$, $n_f(E)$, and $\sigma_f(E)$ are the desired number of incident neutrons, the number of fission events detected by fission chamber, and the fission cross sections of ^{238}U for corresponding neutron energy E respectively ϵ_{det}

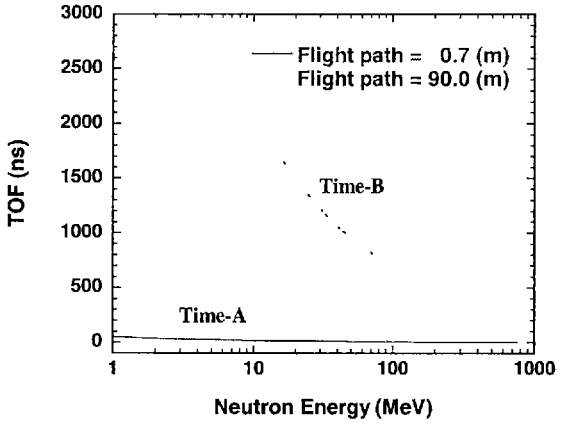

Fig. 7 Estimations of Time-A and Time-B.

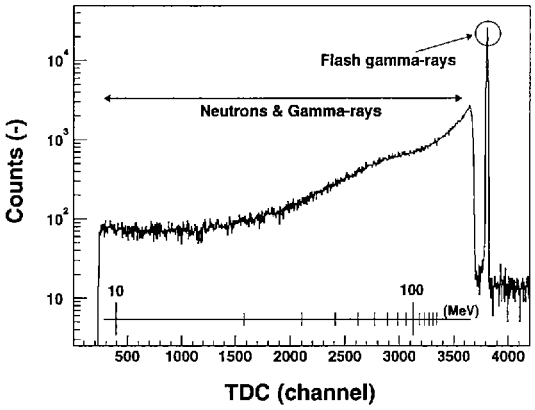

Fig. 8 Typical TOF spectrum between the Target-4 and NE213

is the detection efficiency of the fission chamber, and ρ_f is the arial density of the number of atoms of fissionable material deposited on the foil in the chamber (see ref[15]). $n_f(E)$ was also determined by TOF. Measured fission cross sections[19,20] were used as $\sigma_f(E)$.

3. Outgoing neutron energy spectra

Electron-equivalent light-unit spectrum was obtained from the charge-integration spectrum of NE213 based on calibration analysis The example light-output spectra that were normalized by the number of incident-neutrons and were subtracted background (sample-out) spectra are shown in **Fig. 9** at 90 - 110 MeV neutron-incidence for the iron target.

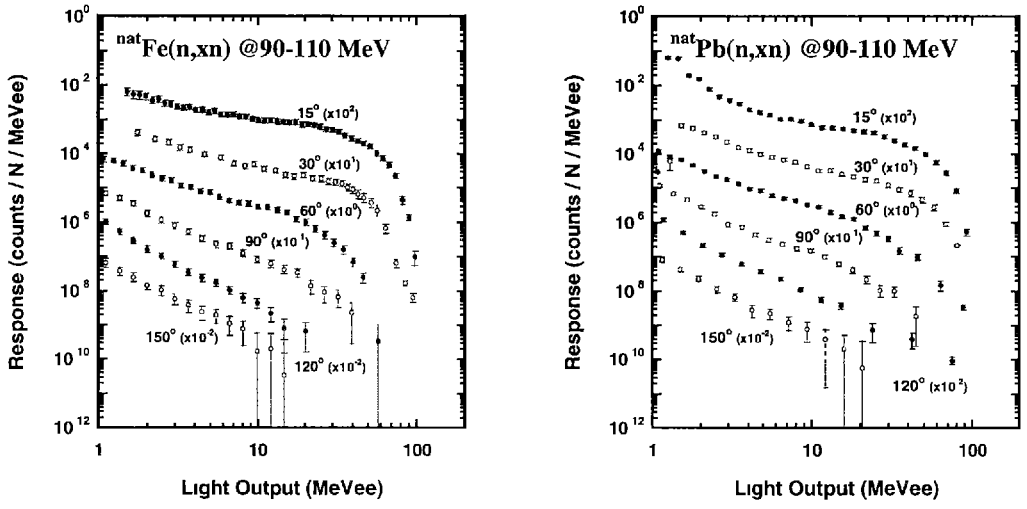

Fig. 9 Example light-output spectra of NE213 at 90 - 110 MeV neutron-incidence for the iron sample

Outgoing-neutron energy spectra were determined by unfolding measured light-output spectra with response functions of NE213 The FERDO[21] unfolding code was used to get optimal neutron energy spectrum. The SCINFUL-R[22] calculations, that were adjusted to reproduce measurements[23] by light attenuation and reduction factors, were used as response matrix elements for all neutron detectors Examples of response functions are shown in **Fig. 10**

Gaussian shape window functions that determined energy resolutions of outgoing-neutron energy spectrum were assumed to be 10 $\sim$ 80 %, and the lowest light-output thresold levels were fixed around 2 MeVee in the unfolding process. Because neutron detectors were not large enough to differentiate neutron energy above 120

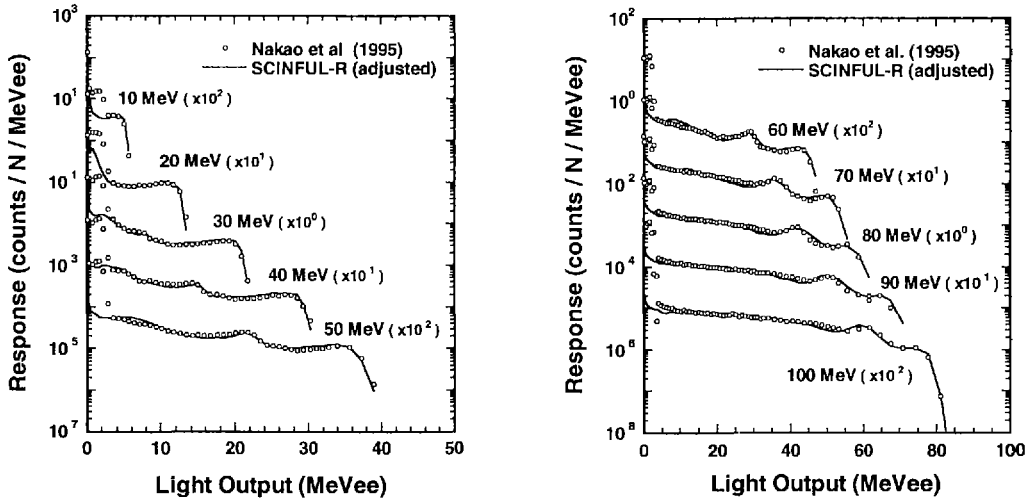

Fig. 10 Example neutron response functions of NE213 for 10 - 100 MeV used in this unfolding process.

MeV in respect to charge-integration of NE213, data analysis was performed up to around this energy. Obtained double-differential cross sections were shown in **Fig. 11** at 90 - 110 MeV neutron-incidence for the iron sample and the lead sample with calculations by the GNASH code DDX can be calculated basing on the Kalbach and Mann's systematics[24] with the exciton pre-equilibrium model and the Hauser-Feshbach statistical evaporation model in this code

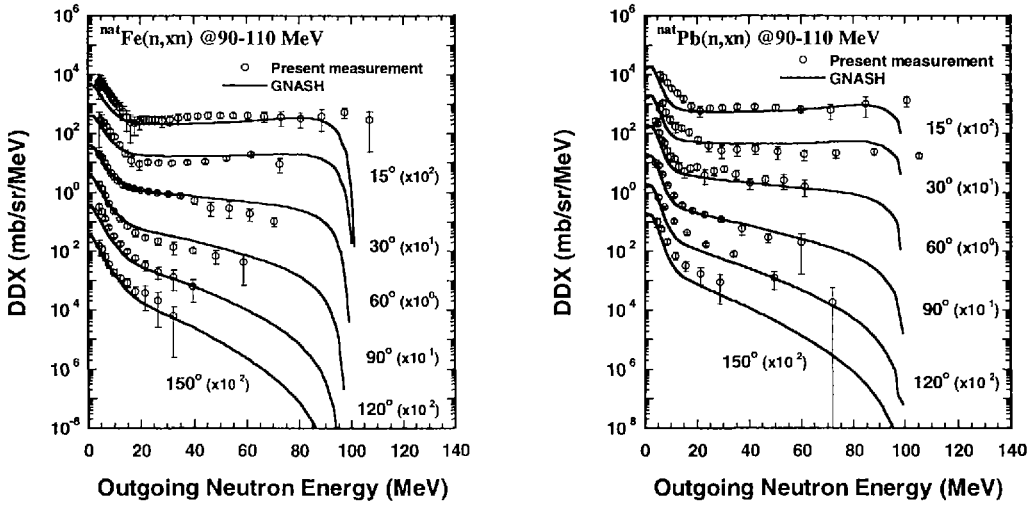

Fig. 11 Preliminaly DDX for iron and lead sample with calculations at 90 - 110 MeV

It must be known that these approach and results are preliminary, because calculational response functions were used in this analysis Neutron detectors usually have thier own chracters due to the depletion of the NE213 and the transmission efficiency of the light signal to the photomultiplier, and a slight difference of response functions are tend to affect the final neutron energy spectrum Response functions for neutron detectors used in this measurement should be used in the unfolding process radically.

IV. Summary

Double-differential cross sections were measured for (n,xn) by using of spallation neutrons as incident-particles. Incident-neutron energy was determined by TOF between the neutron source and neutron detectors Preliminary DDXs were obtained up to about 100 MeV by unfolding charge-integration spectrum of NE213 with calculational response functions, and were compared with calculations by the GNASH code

Recently, response functions have been measured for all NE213s used in the present measurement by using of spallation neutrons, and the analysis is now being proceeded. It will be hoped to get pure measurements by using of measured response functions in the unfolding process

References

1) P. G. Young, E D. Arthur, and M. B. Chadwick, LA-6947 (1977) ; LAUR-88-382 (1988).
2) K. Niita, H. Takada, S. Meigo, and Y. Ikeda, *J. Nucl. Instrum. Methods Phys. Res.*, **B184**, 406 (2001).
3) K. Niita, S. Chiba, T. Maruyama, H Takada, T. Fukahori, Y. Nakahara, A. Iwamoto, *J. Phys. Rev.* **C52**, 2620 (1995)
4) B. E. Bonner, J E Simmons, C R Newsom, P. J. Riley, G. Glass, J C. Hiebert, Mahavir Jain*, and L. C Northcliffe, *J. Phys. Rev.* **C18**, 1418 (1978)
5) S. Cierjacks, Y. Hino, F. Raupp, L. Buth, D Filges, P. Cloth, and T W. Armstrong, *J. Phys. Rev* **C36**, 1976 (1987)
6) M. M. Meier, D A Clark, C A Goulding, J B. MaClelland, C E Moss, and W. B. Amian, *J. Nucl Sci. Eng.*, **102**, 310 (1989).
7) W. Scobel, M. Trabandt, M. Blann, B A Pohl, B. A. Remington, R C Byrd, C C. Foster, R. Bonetti, C. Chiesa, S M Grimes, *J. Phys. Rev.* **C41**, 2010 (1990).
8) S. Stamer, W. Scobel, W. B. Amian, R. C Byrd, R. C. Haight, J. L. Ullmann, R. W. Bauer, M. Blann, B. A. Pohl, J. Bisplinghoff, R. Bonetti, *J. Phys Rev* **C47**, 1647 (1993)
9) W. B. Amian, R. C. Byrd, D A. Clark, C A Goulding, M. M. Meier, G L. Morgan, and C. E. Moss, *J. Nucl. Sci Eng.*, **115**, 1 (1993).
10) T. Nakamoto, K Ishibashi, N Matsufuji, N. Shigyo, K. Maehata, S. Meigo, H. Takada, S. Chiba, M. Numajiri, T. Nakamura, Y. Watanabe, *J Nucl. Sci Technol.*, **32**, 827 (1995).
11) S. Leray, F. Borne, S. Crespin, J. Frehaut, X Ledoux, E. Martinez, Y. Patin, E. Petibon, P. Pras, A Boudard, R. Legrain, Y. Terrien, F. Brochard, D. Drake, J. C. Duchazeaubeneix, J. M. Durand, S. I. Meigo, G. Milleret, D. M. Whittal, W Wlazlo, D. Durand, C Le Brun, F. R. Lecolley, J. F. Lecolley, F. Lefebvres, M. Louvel, C Varignon, F Hanappe, S Menard, L Stuttge, J. Thun, *J. Phys. Rev* **C65**, 044621 (2002)
12) A. Marcinkowski, R. W. Finlay, G Randers-Pehrson, C. E. Brient, R Kurup, S. Mellema, A. Meigooni, R. Tailor, *J Nucl. Phys* , **A402**, 220 (1983)
13) E. L Hjort, F. P. Brady, J R. Drummond, B. McEachern, J H. Osborne, J. L Romero, D S. Sorenson, and H H K Tang, *J. Phy. Rev* , **C53**, 237 (1996)
14) P. W Lisowski, C. D. Bowman, G. J Russell, and S A Wender, *J. Nucl. Sci Eng* , **106**, 208 (1990)
15) S. A. Wender, S Balestrini, A Brown, R C Haight, C. M Laymon, T M Lee, P W Lisowski, W. MacCorkle, R O. Nelson, W Parker, and N. W Hill, *J Nucl Instrum Methods Phys Res* , **A336**, 226 (1993).
16) M. Moszynsky, et al , *J Nucl. Instrum Methods* , **A343**, 563 (1994)
17) G Dietze, H Klein, *J Nucl Instrum Methods* , **193**, 549 (1982)
18) R. A. Cecil, B D Anderson, and R Madey, *J Nucl Instrum Methods* , **161**, 439 (1979).
19) P. Staples, P W Lisowski, and N W Hill, Presented in APS/AAPT Conference, Washington, April 18-12, 1995, *Bull Am Phys Soc* , **40**, 962 (1995)
20) V I. Goldanskiy, V. S. Penkina, and E Z Tarumov, *ZETP (Sov J of Experimental and Theoretical Physics)*, **29**, 778 (1955)
21) B. W Rust, D. T Ingersoll, and W R Burrus, "A user's manual for the FERDO and FERD unfolding codes", Oak Ridge National Laboratory ORNL/TM-8720, (1983)
22) S. Meigo, *J Nucl. Instrum Methods Phys Res.*, **A401**, 365 (1997)
23) N. Nakao, T Nakamura, M Baba, Y Uwamino, N. Nakanishi, H. Nakashima, S Tanaka, *J Nucl Instrum Methods Phys. Res.*, **A362**, 454 (1995).
24) C. Kalbach, *J Phys. Rev.* **C37**, 2350 (1988)